Pressure induced superconductivity in molecular TTF(Pd(dmit) 2)2

L. Brossard, M. Ribault, Lydie Valade, P. Cassoux

Classification
Physics Abstracts
63.20K — 64.70 — 72.15N — 72.80L — 74.70L

Pressure induced superconductivity in molecular $TTF(Pd(dmit)_2)_2$

L. Brossard (1), M. Ribault (1), L. Valade (2) and P. Cassoux (2)

(1) Laboratoire de Physique des Solides associé au C.N.R.S., Université Paris-Sud, Bât. 510, 91405 Orsay, France
(2) Laboratoire de Chimie de Coordination C.N.R.S., 31077 Toulouse, France

(*Reçu le 11 octobre 1988, révisé le 19 janvier 1989, accepté le 10 février 1989*)

Résumé. — Les instabilités 1D de type Spin Peierls et Onde de Densité de Spin sont absentes du diagramme de phase (température, pression) de la phase monoclinique centrée de $TTF(Pd(dmit)_2)_2$. A basse pression, une localisation graduelle des porteurs apparaît à $70\ K < T < 250\ K$ et l'état fondamental est un semi-conducteur à bande interdite faible ou un semi-métal. A haute pression, une supraconductivité sale s'impose en dessous de 6 K et qui semble compatible avec des Ondes de Densité de Charge observées à 1 bar.

Abstract. — Analysis of the temperature-pressure phase diagram of the centered monoclinic phase of $TTF(Pd(dmit)_2)_2$ reveals the absence of 1D instabilities such as Spin Peierls and Spin Density Wave ground states. At low pressures and between 70 and 250 K, a gradual localization of the carriers leads to a small gap semi-conductor or to a semi-metal. At high pressures, a dirty superconductivity sets in below 6 K and seems compatible with Charge Density Wave instabilities observed at 1 bar.

1. Introduction.

Up to now, 5 families of organic compounds are known to undergo a superconducting ground state : 1) the quasi 1D Bechgaard salts composed of π-donor organic and symmetric molecules of TMTSF and closed-shell inorganic anions (ClO_4, PF_6...) with a superconducting temperature $T_c \sim 1$ K [1] ; 2) the 2D $(BEDT\text{-}TTF)_2X$ salts with a relatively « high » T_c (8 and 10 K with $X = I_2$ and $Cu(SCN)_2$, respectively [2] ; 3) the $(DMET)_2AuX_2$ (with $X = CN$, I, Br, Cl) [3], and the $(DMET)_2X$ salts (with $X = I_3$, I_2Br, IBr_2 [3, 4] characterized by asymmetric donors resulting from the hybrid structure of TMTSF and BEDT-TTF, and with $T_c \sim 0.5$ K ; 4) the $(MDT\text{-}TTF)_2AuI_2$ salt [5] also based on asymmetric donor but with $T_c = 3.5$ K at 1 bar ; 5) the $D(M(dmit)_2)_n$ compounds based on organo-sulfur donor molecules D and acceptor metal complexes $M(dmit)_2$ ($dmit_2$ = 1,3-dithia-2-thione-4,5-dithiolato) [6, 9]. These $D(M(dmit)_2)_n$ two-chain charge-transfer salts show various electronic properties depending on the nature of the metal M, of the donor D and on the stoichiometry n. For example, $TTF(Ni(dmit)_2)_2$ and $(CH_3)_4N(Ni(dmit)_2)_2$ become superconductors under a moderate pressure of 7 kbar ($T_c = 1.62$ K [7] and 5 K [8], respectively). On the opposite, at

room temperature, $TTF(Pt(dmit)_2)_2$ is a semiconductor and $TTF(Pd(dmit)_2)_2$, although exhibiting a higher conductivity compared to its Ni counterpart, shows a metal semiconductor transition at 1 bar and at high temperature [9].

The aim of this work was to specifically study the $TTF(Pd(dmit)_2)_2$ compound in order to see if the pressure-effect could suppress the « metal-insulator » transition and induce a superconducting ground state. Moreover, since well known quasi-1D instabilities were not observed in the temperature-dependent conductivity behavior of $TTF(Ni(dmit)_2)_2$ at 1 bar, it was expected that the study of the Pd derivative could help to elucidate two unsolved questions : i) what is the dimensionality and ii) what is the charge transfer of these salts.

Part 2 is devoted to the experimental aspects of this work (pressure apparatus and samples) ; experimental results as a function of the pressure range are analysed in section 3 ; part 4 is devoted to the discussion of the phase diagram and to conclusion.

2. Experimental.

2.1 APPARATUS. — A. C. low frequency (77 Hz) longitudinal resistivity measurements were performed *via* the standard 4 point method : the samples ($4 \times 0.15 \times 0.05$ mm^3) were fixed through 4 annealed gold wires ($\varnothing$ 25 μ) glued with silver paint on evaporated gold precontacts. The other extremities of the gold wires were soldered on copper ($\varnothing$ 0.2 mm) feedthroughs insulated into pyrrophylite. The contact resistances typically range between 1 to 10 Ω depending on the pasting quality. In general, they degrade continuously with decreasing temperature. Care was taken that measurements were performed at constant current (100 μA) when decreasing the temperature ; at $T < 4.2$ K measurements were done at 10 μA in order to avoid Joule heating of the sample in the case of damaged current contact resistance. Likewise the decreasing temperature runs were controlled by subsequent increasing runs using a 10 μA constant current.

Two types of obturators were used : CuBe one for pressures lower than 15 kbar and maragin-steel above. The obturator was fitted into a teflon cell filled with a fluid used as pressure transmitting and sample thermalising medium. Since the pressure bombs used were clamp systems, it was necessary to evaluate accurately the loss of pressure during the cooling process between 300 K and just below the freezing temperature of the medium. Hence a heavily dopped (10^{18}) « InSb : Te » manometer was mounted beside the sample inside the teflon cell : Firstly, this allows us to monitor the room temperature pressure since, with Te as dopant, pressure is limited only by a phase transition at 25 kbar instead of 23 kbar with undoped InSb [10]. In the second place, in such a heavily dopped narrow band gap semiconductor, the temperature dependence of the resistivity is very small and is pressure independent [11]. Thus the low temperature pressure was determined with an accuracy better than 200 bar (1 % at 20 kbar).

The clamp heat-treated Cu-Be vessel was fixed at the bottom of the mixing chamber of a dilution refrigerator. Since the freezing temperature of the medium was relatively high (250-300 K) in the high pressure measurements, care was taken to always insure a very slow cooling process between 300 and 77 K (12 K/hour) : firstly, this avoids damage of the contact resistances during the freezing of medium. In the second place, this minimizes induced strains on the sample from local stresses resulting from non perfect hydrostatic pressures. Thus resistivity curves of the samples were obtained without noticeable jumps.

2.2 SAMPLES. — Black shiny needles of $TTF(Pd(dmit)_2)_2$ were prepared [6] by slow interdiffusion of saturated solutions of $(TTF)_3(BF_4)_2$ and $(n\text{-}Bu_4N)(Pd(dmit)_2)$. X-ray diffraction measurements at 1 bar and at 300 K lead to a C-centered ordered monoclinic structure isostructural with the $TTF(Ni(dmit)_2)_2$ one (cf. Fig. 1) : it consists of segregated

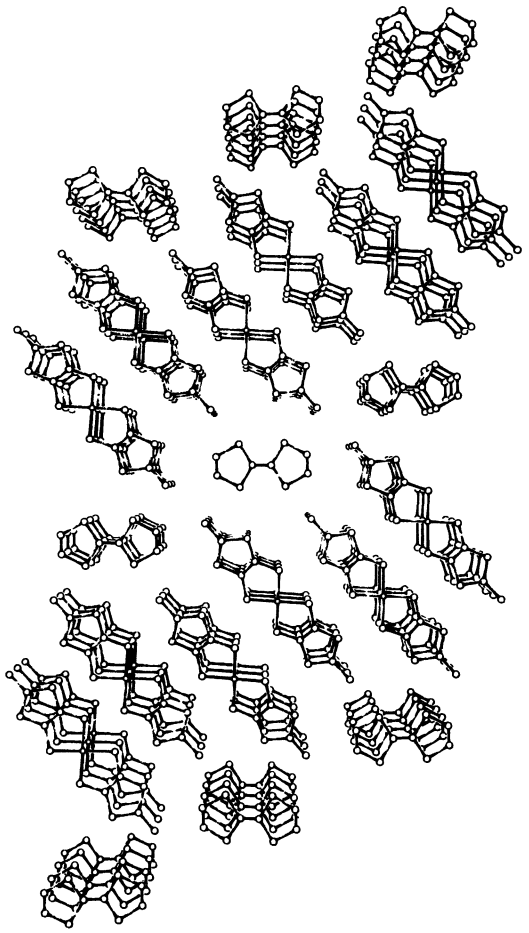

Fig. 1. — Perspective view along (010) of the centered monoclinic unit cell of $TTF[M(dmit)_2]_2$ with M = Ni, Pd.

regular stacks of TTF and $Pd(dmit)_2$ entities along (010) ; the spacing between stack sites is b = 3.60 Å, but due to different tilted orientations, the interplanar spacing is 3.44 Å within the $Pd(dmit)_2$ stack and 3.52 Å within the TTF one [12]. These spacings are significantly shorter than for the Ni derivative (b = 3.73, 3.55 and 3.65 Å respectively) [13]. It has to be pointed out that this b-axis shrinking is opposite to the atomic radius expansion from Ni to Pd [14]. On the other hand, the unit cell parameters a and c in the plane perpendicular to (010) do increase, but only by 1 % ; this increase remains 10 times smaller than the relative increase of the atomic diameters from Ni to Pd. These features lead to stronger intermolecular intra and interstack S-S interactions and thus to a network which seems to be of higher dimensionality than for the Ni analog.

Three crystalline phases have been observed at different temperatures and ambient pressure in the case of needle-like crystals of $TTF(Pd(dmit)_2)_2$: a high temperature monoclinic and weak metallic α-phase, a low temperature triclinic and semi-conducting β-phase, and a triclinic and semi-conducting γ-phase obtained upon warming the β-phase back at room temperature [12] ; the crystallographic transition from the α- to the β-phase is gradual, begins at 240 K and is not achieved at 180 K : it is associated with a minimum of the

resistivity around 220 K and is characterized by a temperature hysteresis which increases when the sample is longer kept at low temperatures [12].

Other needles of the same batch, however, do not exhibit any resistivity hysteresis under thermal cyclings ; these single crystals are not discernible from the preceding ones under optical microscope investigations ; X-ray diffraction crystal structure determinations have corroborated that these crystals are not undergoing any structural phase transition down to 77 K [12]. Table I [12] summarized the crystal data of $TTF(M(dmit)_2)_2$ with M = Ni, Pd at 1 bar. The so-called α'-phase thus seems to keep the C-centered monoclinic structure and stay isostructural with the Ni analogue system down to low temperatures. Electronic properties of this α'-phase constitute the main part of this work.

Table I. — *Crystal data of* $TTF[X(dmit)_2]_2$ *at* 1 bar [12].

X	a	b	c(Å)	α	β	γ(°)	V(Å^3)	Space group ($Z = 4$)
Ni (293 K)	46.22 (3)	3.732(2)	22.86 (1)	90	119.3 (1)	90	3 439	C2/c
Pd α'(293 K)	46.794(1)	3.608(1)	23.109(5)	90	119.55(2)	90	3 394	C2/c
α (293 K)	46.703(8)	3.596(3)	23.085(4)	90	119.48(2)	90	3 374	C2/c
β (100 K)	46.49 (2)	3.553(4)	22.92 (1)	89.9 (1)	119.15(4)	90.1 (1)	3 307	$P\bar{1}$
γ (293 K)	46.688(6)	3.605(2)	23.054(4)	89.94(8)	119.48(1)	90.07(8)	3 378	$P\bar{1}$

3. Results and analysis.

3.1 ROOM TEMPERATURE PRESSURE DEPENDENCE. — As shown in figure 2, the resistance of $TTF(Pd(dmit)_2)_2$ is continuously decreasing with increasing pressure up to 24 kbar : the initial slope d Log R/dP is equal to -0.10/kbar instead of -0.18/kbar for the Ni salt. The initial resistance ($\rho_0 = 1\,300$ μΩ cm) is divided just by 3 at 17.5 kbar, whereas the same result is already obtained at 7.5 kbar for the Ni salt ($\rho_0 = 3\,300$ μΩ cm). From the preceding discussion (cf. 2.2 and Tab. I), it appears that the Ni salt is more compressible than the Pd one : indeed since the unit cell parameter b along the stack is equal to 3.73 and 3.60 Å respectively, an increasing pressure will much more increase the overlap of sulfur orbitals along the b direction — and hence the conductivity — in the Ni salt case compared to the Pd one. Yet, whereas at 7 kbar the Pd salt is still two times more conductive than the Ni one, at lower temperatures the latter becomes superconducting [7] and the former still remains semiconducting as we shall see.

3.2 DIFFERENCES BETWEEN THE α AND α'-PHASES. — The temperature dependence of the resistance of the α- and α'-$TTF(Pd(dmit)_2)_2$ phases are quite different not only at 1 bar as discussed in 2.2, but also at high pressures as shown in figure 3 : at 24 kbar, the resistance of the α'-phase varies linearly with temperature down to 100 K, then shows an S shape and finally exhibits a residual resistance plateau below 10 K above the complete superconducting transition (T_c onset = 5.93 K). This behaviour reminds the overall resistivity dependence of the Ni salt at 7 kbar (with T_c onset = 1.95 K) [7].

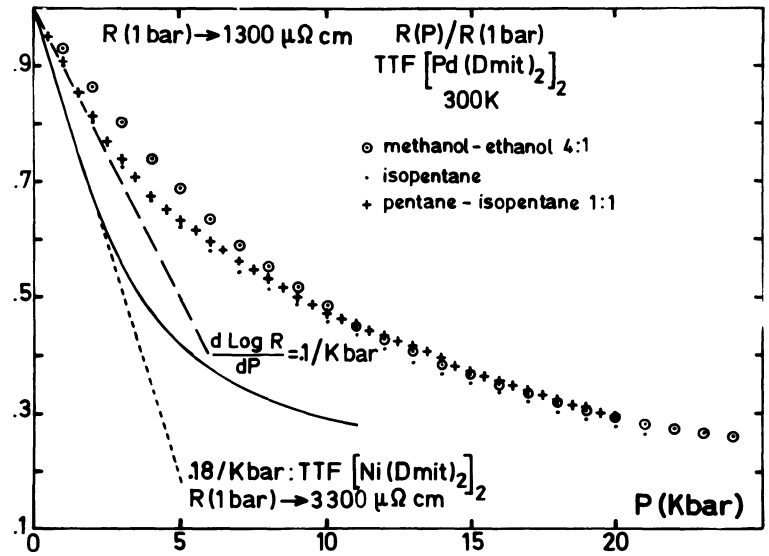

Fig. 2. — Compared pressure dependence of the normalized resistances of TTF[Pd(dmit)$_2$]$_2$ and TTF[Ni(dmit)$_2$]$_2$ at 300 K.

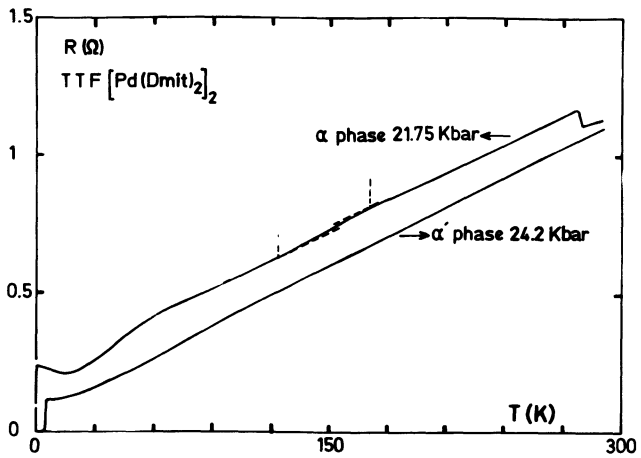

Fig. 3. — Compared temperature dependence of the resistances of α and α'-TTF[Pd(dmit)$_2$]$_2$ phases at high pressures (measured at low temperatures).

On the other hand, the resistance of the α-phase shows an anomaly between 165 and 135 K at 22 kbar and between 170 and 140 K at 19 kbar (not shown). This may be attributed to the phase transition from monoclinic to triclinic which occurs below 240 K at 1 bar. Despite the lower symmetry of the low temperature phase, it is to be noticed that the resistance decreases during the phase transition. At lower temperatures, the resistance shows a better marked S-shape than for the α'-phase but reaches a minimum whose temperature decreases with increasing pressure (cf. Fig. 4). Then, superconducting transitions occur but at lower temperatures than for the α'-phase.

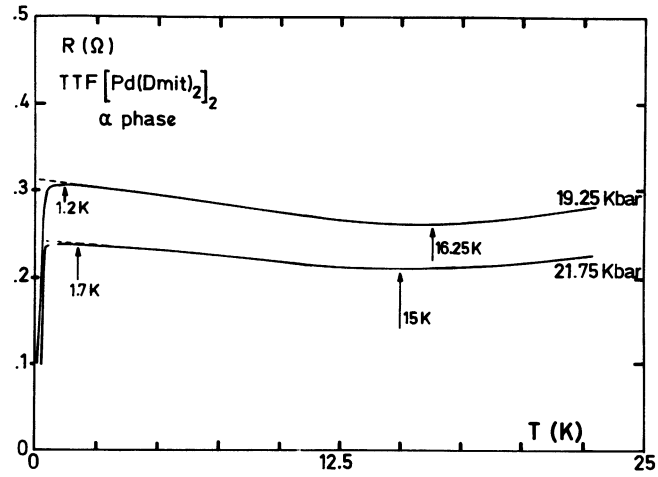

Fig. 4. — Low temperature dependence of the resistance of α-TTF[Pd(dmit)$_2$]$_2$ at high pressures (measured at low temperatures).

3.3 PHASE DIAGRAM OF THE α'-PHASE.

3.3.1 *At high pressures* ($P > 20$ kbar). — Figure 5 shows the superconducting transitions obtained on the same sample at three pressures : only one transition (at 24 kbar) is complete (T_c onset = 5.93 K ; T_c at midheight = 5.55 K ; $\Delta T_c = 0.64$ K). The other two are not : the resistance drop at 22 kbar (T_c onset = 6.05 K) and at 20.7 kbar (T_c onset = 6.42 K) is respectively equal to 71 and 35 % of the normal state values. For the three pressures, the temperature dependences of the resistances are similar to the Ni salt at 7 kbar [7] i.e. : i) linear over a wide temperature range (between 100 and 250 K) and ii) characterized by a residual resistivity plateau : this is the signature of inelastic scatterings for the carriers that are induced by non-magnetic defects. This feature contrasts with the linear temperature dependent resistivity of $(TMTSF)_2PF_6$: this linear variation is observed just above

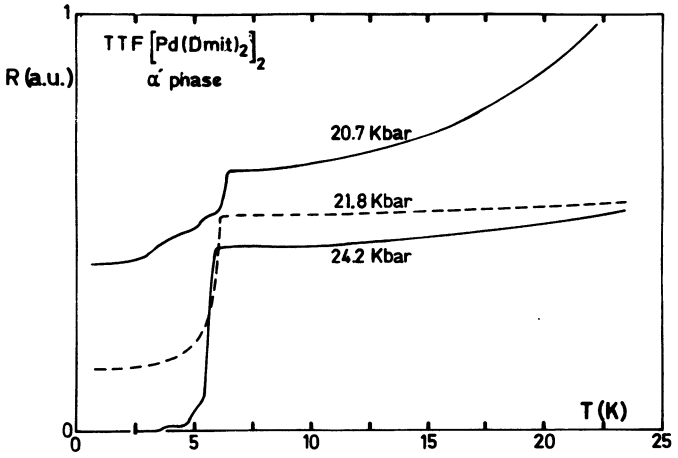

Fig. 5. — Superconducting transitions of α'-TTF[Pd(dmit)$_2$]$_2$ at high pressures (measured at low temperatures).

T_c and at pressures greater than the tricritical point pressure [1] and is attributed to dominant antiferromagnetic (AF) fluctuations [15]. Hence, we can derive from this discrepancy between the Beechgaard salt and the TTF(M(dmit)$_2$)$_2$ systems that if these compounds are relevant from a clean superconductivity, it must arise from a classical electron-phonon picture ; on the other hand, if the superconductivity is dirty, the dominant electron-impurity scatterings can mask the AF fluctuations which could induce the superconducting ground state.

The slope of the superconducting onset temperature *versus* pressure d Log T_c/dP is equal to $-\alpha = -(2.6 \pm 0.2)\ 10^{-2}$/kbar. In order to find the origin of the relatively high T_c value of TTF(Pd(dmit)$_2$)$_2$, it has been attempted to correlate its pressure dependence with the strong electron-phonon coupling model of McMillan [16] : this leads to a critical pressure above which superconductivity should appear of 40 kbar, which is obviously too high. Hence, as in the case of (TMTSF)$_2$PF$_6$, the McMillan model is not relevant in order to describe the superconductivity of these compounds. It is to be pointed out that the slope d Log T_c/dP is equal to -3.5×10^{-2}/kbar for (TMTSF)$_2$PF$_6$, by using Orsay and Bell laboratories data [1] ; owing to the low pressure SDW state and AF fluctuations, the decrease of T_c by pressure is then stronger than in the Pd salt. This discrepancy between (TMTSF)$_2$PF$_6$ and α'-TTF(Pd(dmit)$_2$)$_2$ suggests a contrario the absence of any SDW state in close vicinity with superconductivity in the last compound (cf. 3.3.2) ; also, it seems plausible that the AF fluctuations are not the dominant mechanism leading to superconductivity even above 20 kbar where superconductivity sets in directly from the stabilized metallic state.

Superconducting properties of α'-TTF(Pd(dmit)$_2$)$_2$ were confirmed by applying a magnetic field H parallel to the a direction (i.e. perpendicular to the plane b-c of the needle). The critical fields H_{c_2} were determined as the onset of superconductivity in decreasing magnetic field [17]. Figure 6 shows the temperature dependence of the reduced critical field $h_{c_2} = H_{c_2}(T)/H_{c_2}(0)$ at 20.7 and 24 kbar. A high temperature linear regression leads to $T_c = 6.53$ and 5.63 K respectively, in fair agreement with the experimental values. Since the superconducting transitions are rather broad, $H_{c_2}(0)$ can be calculated within the dirty limit approximation [18] as $H_{c_2}(0) = 0.69\ T_c(dH_{c_2}/dT)_{T_c}$; the values thus obtained 980 and 865 G, are in close agreement with the experimental ones (1 020 and 930 G at 20.7 and 24 kbar, respectively). Our dirty superconductivity assumption is reinforced by the fact that, if the samples were clean, we should have observed a positive curvature of $H_{c_2}(T)$ below T_c [19] resulting from the anisotropy of FS ; as shown in figure 6, such a positive curvature is not experimentally observed. The same reduced slope $dh_{c_2}/dt = -1.38$ with $t = T/T_c$ is obtained for both pressures. Thus, the $h_{c_2}(t)$ curve deviates from a purely parabolic law for which $dh_{c_2}/dt = -2$. Now, due to the lack of measurements of the thermodynamic critical field $H_c(T)$ and of the molar volume in the 20 kbar pressure range, no precise values can be derived for the electronic specific heat coefficient γ [20] and for the band structure density $N(0)$ of electronic states [21]. Nevertheless a very crude estimation of : i) $H_c(0)$ (~ 220 G $= 37\ T_c$) by analogy with relaxed (TMTSF)$_2$ClO$_4$ [22] and of ii) the molar volume (by taking a decrease of 1 % per kbar from the 1 bar value) lead to $\gamma = 10$ mJ/mole K^2, which is very close to the corresponding value obtained for (TMTSF)$_2$ClO$_4$ by calorimetric measurements [22].

3.3.2 *At low pressure* ($P < 20$ kbar). — Plots of the normalized resistivity *versus* $1/T$ at $P < 17$ kbar were published elsewhere [23] : the resistivity exhibits at first sight a broad minimum around a high temperature T_p (240 ± 20 K at 1 bar), the value of which decreases with increasing pressure (initial slope $dT_p/dP = -7$ K/kbar). Despite the uncer-

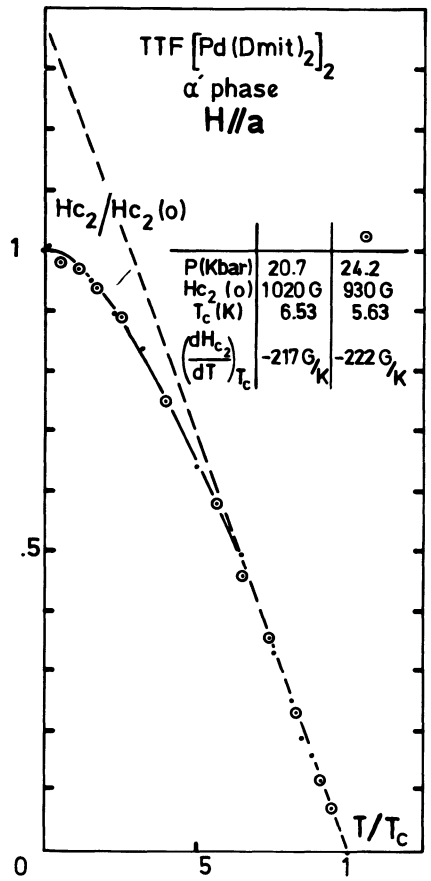

Fig. 6. — Temperature dependence of the reduced critical field $h_{c_2} = H_{c_2}(T)/H_{c_2}(0)$ at two pressures. The magnetic field H is directed along the a axis of the unit cell of α'-TTF[Pd(dmit)$_2$]$_2$. The $H_{c_2}(0)$ values are experimental. The values of T_c and of $(dH_{c_2}/dT)_{T_c}$ were obtained by high temperature linear regression.

tainty (40 K at 1 bar) on the absolute value of T_p, this resistivity minimum is in fact not so broad, since its uncertainty should correspond to 4 K at 24 K. No discontinuity can be detected in the slope d Log R/d$(1/T)$, which shows only a maximum around a temperature T_s (110 ± 15 K at 1 bar) at the inflexion point of each curve (initial slope $dT_s/dP = -3$ K/kbar). Hence, it seems convenient to consider the T_s values as the temperatures below which the « metal-semiconductor » transition takes place ; localization of the carriers begin between T_p and T_s and the nature of the semiconducting state must be determined at $T < T_s$: below 9 kbar, a. c. resistivity measurements were not performed at sufficient low temperatures, due to the increasing impedance of the samples. At 15 kbar (and above) correct a. c. measurements were performed down to 4 K (and below) : at 15 kbar, T_p and T_s are respectively equal to 110 and 45 K, and the only temperature range where an activation energy Δ can be defined is located around 45 K, i.e. at T_s. Hence, the pressure dependence of Δ has been tentatively defined around each T_s value : the ratio $2\Delta/T_s$ remains constant (13 ± 0.2) up to 9 kbar, drops to 7 at 15 kbar and reaches the mean field value at 16 kbar. In an activation energy framework, these 2Δ values could be considered as the

maximum values reached by the pressure decreasing gap ($2\Delta = 130$ meV at 1 bar, which is a value 6 times larger than the gap measured on the α-phase at 1 bar [9]). However, the temperature range over which Δ can be defined is quite narrow (30 K at 1 bar) and is narrowing as pressure increases ; furthermore, if the gap is temperature dependent, Δ has been defined at too high temperatures and such a derivation is not relevant.

D. c. resistivity measurements are carried out at 1 bar and down to 4 K in order to confirm the general behaviour observed at 15 kbar, i.e. the impossibility to determine a gap in this compound. If this is the case, this will signify that the low pressure ground state is rather a semi-metal than a semiconductor. This will be published later on.

Since the classical activation energy picture does not provide a satisfactory description of the resistivity variations, a tentative plot of the normalized resistivity Log (R/R_0) *versus* $T^{-1/4}$ is shown in figure 7, where R_0 is the 1 bar resistance : it is clear that here also a 3D short range hopping model [24] does not apply — whatever the pressure —, since no plot is linear over a sufficiently large temperature range. The same result is obtained in 2D [25] and 1D [26] short range hopping models, by plotting Log (R/R_0) *versus* $T^{-1/3}$ and $T^{-1/2}$ respectively.

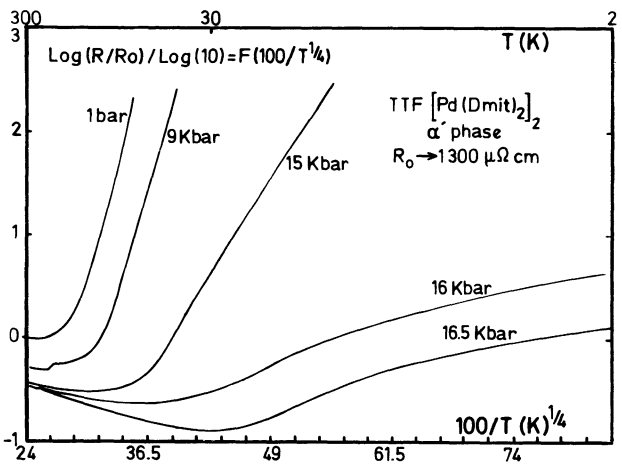

Fig. 7. — Plot of the low pressure normalized resistance of α'-TTF[Pd(dmit)$_2$]$_2$ phase following Log $R \sim 1/T^{1/4}$ (3D short range hopping). Indicated pressures were measured at low temperatures.

No sign of superconductivity is observed at 16 kbar down to 80 mK ; from 16.5 to 17.5 kbar, the superconducting onset temperature T_c increases from 0.2 to 1.6 K, whereas the respective values of T_p ($\sim$ 32 K) and T_s ($\sim$ 15 K) do not vary significantly. It is to be pointed out that the resistance ratio $RR = R(300) - R(T_p)/R(T_p)$ is increasing with pressure from 0.04 at 1 bar to 110 at 24 kbar, showing the increasing metallic character of the conductive state. At 19.2 kbar, the superconducting onset temperature T_c was measured by the three-contact method only ; thus it is difficult to determine the T_p and T_s values owing to the temperature drift of one contact resistance. Nevertheless, it seems plausible to assume they are close to 11 and 9 K respectively so that the $T_p(P)$ and $T_s(P)$ variations converge on a tricritical point in the phase diagram (cf. 3.3.3 and Fig. 9).

Figure 8 shows the variations of the resistivity *versus* $T^{1/2}$ from 16 to 17.5 kbar : a linear part is observed at 16 kbar between 0.5 and 2 K suggesting that 3D weak localization [27] could occur in the sample. But magnetic fields were not applied to confirm without doubt this

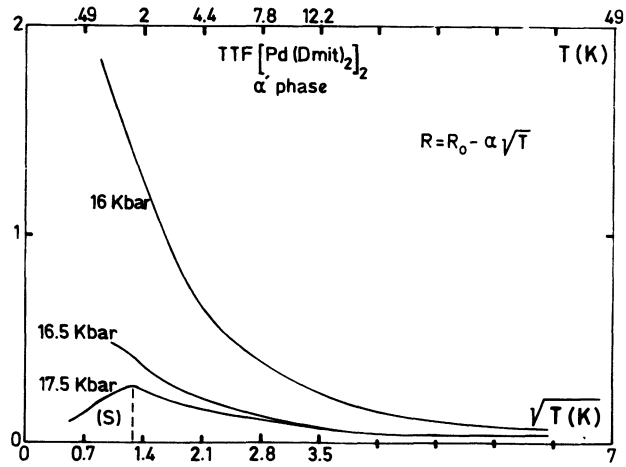

Fig. 8. — Variation of the resistance of α'-TTF[Pd(dmit)$_2$]$_2$ *versus* $\sqrt{T}$ at 16, 16.5 and 17.5 kbar (measured at low temperature). The linear part observed between 0.5 and 2 K suggests a possible 3D weak localization at 16 kbar.

possible behaviour. On the other hand, a similar plot of the resistivity *versus* Log T, does not show any linear variation. Hence, weak localization — if there is any — has not a 2D character [28].

Plots of Log R *versus* $1/T$ at 15 kbar (down to 4 K), 16 kbar (down to 80 mK), 16.5 and 17.5 kbar (down to T_c) are continuous and show no detectable variations in their curvature below T_s : this removes the hypothetical existence of a low temperature SDW ground state which could appear in a narrow pressure window in close vicinity with the superconducting state.

3.3.3 *Phase diagram.* — The pressure dependence of T_p, T_s and T_c are displayed in figure 9, which shows the entrance of superconductivity into the semiconducting ground state : it is of interest to notice that the slope d Log T/dP is equal to $-\alpha = -(2.6 \pm 0.2)\, 10^{-2}$/kbar not only for the pressure dependence of the superconducting onset temperature T_c (at $P > 20$ kbar), but also for the low pressure variations of T_p and T_s. This accounts for the remarkable invariability of the ratio $T_p(P)/T_s(P) \sim 2$ up to 9 kbar. Moreover, the fact that the same slope is observed in the well established superconducting regime ($P > 20$ kbar) as well as in the semiconducting ground state ($P < 9$ kbar) means that the same exponential pressure dependence governs not only the superconducting condensation but also the carrier localization. Hence, the same basic physical process leading to the semiconducting and to the superconducting states is at work at low and high pressures respectively.

The last comment related to this phase diagram concerns the nature of the low pressure ground state : a SDW instability near the superconductivity has been excluded by the preceding discussion. Moreover, low temperature ($T > 7$ K) ESR measurements performed at 1 bar on 10 oriented crystals [23] show no precursor effects to Spin Peierls (SP) transition or to long range AF order just above 7 K ; hence, this suggests that in the low pressure range, the semiconductor does not lead to a Mott insulator at lower temperatures. Nevertheless, such a conclusion has to be confirmed by lower temperature ($T < 7$ K) SQUID static susceptibility and more sensitive ESR measurements that are going to be carried out at 1 bar on one single crystal.

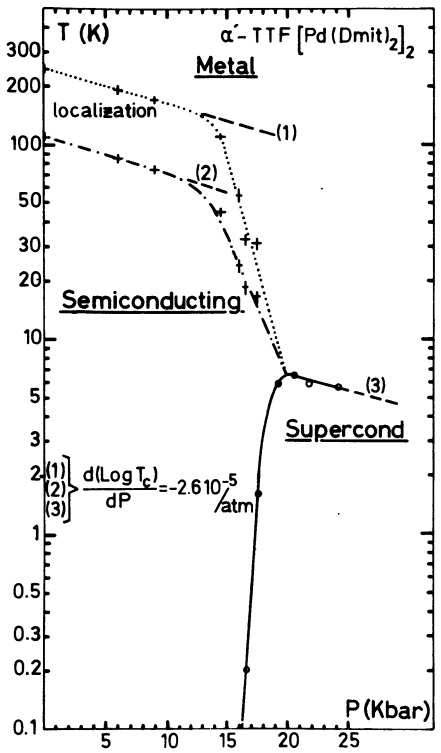

Fig. 9. — Phase diagram of α'-TTF[Pd(dmit)$_2$]$_2$ phase.

4. Discussion and conclusion.

Analysis of the preceding results shows that the molecular TTF(Pd(dmit)$_2$)$_2$ share common features with the Bechgaard salt and related compounds based on PF_6 anion : for example, (TMTTF)$_2PF_6$ presents also a high temperature resistivity minimum at 220 K at 1 bar [29] ; but in this case, a Mott-Hubbard on bond localization of the electron charge is associated with a dimerization at 4 k_F which results from relevant Umklapp processes induced by the PF_6 anion potential ; moreover, at lower temperatures (15 K at 1 bar) a sharp non-magnetic SP ground state at 2 k_F takes place, which constitutes the true thermodynamic phase transition [29]. An increasing pressure reduces the dimerization and thus the Umklapp influence : the repulsive electron-electron interaction along the chain becomes dominant ; this favors AF correlations and the interchain exchange coupling [30] drives a low temperature SDW ground state in close vicinity with superconductivity as observed in (TMTSF)$_2PF_6$ [1]. This sequence SP-SDW-SC is the signature of decreasing influence of Umklapp processes, which are supposed to enhance the 1D AF correlations ; when they are not relevant, then Charge Density Wave (CDW) instabilities may occur [31].

TTF(Pd(dmit)$_2$)$_2$ does not show either low pressure SP or high pressure SDW ground states ; hence, the high temperature freezing of the charge degrees of freedom does not seem to be relevant from Umklapp processes. Moreover, TTF(Pd(dmit)$_2$)$_2$ contains 4 TTF chains per unit cell instead of one single type of conductive chain for the Bechgaard salts. Although it is still unknown which of the three chains - the TTF or/and the two Pd(dmit)$_2$ units — is or are involved in the transport properties, it is clear that they cannot be discussed in the framework of one single band model as is the case for the Bechgaard salts. Hence, the nature of the phase

transition below T_s must be discussed in connection with other experiments, namely previous ESR and recent X-ray diffusion measurements both performed at 1 bar.

Powder ESR spectra show [23] a continuous decrease from 300 to 150 K of the linewidth and of the intensity of a broad conduction electron signal : since no irregularity was detected around T_p, it was suggested [23] that — as in $(TMTTF)_2PF_6$ — the spin degrees of freedom were not freezed around T_p, which was considered as the signature of charge localization only. Below 150 K, a narrower signal appears, the spin susceptibility of which follows a Curie Weiss like behaviour : this was interpreted as spin localization arising from the conduction electrons. In fact, these previous interpretations of powder ESR spectra have to be tempered for two reasons : i) the appearance of the narrow signal below 150 K can also be the result of a charge localisation on one chain [32], ii) recent X-ray diffusion experiments [33] show at high temperatures diffuse lines at $q_1 = 0.5\, b^*$ and $q_2 = \pm 0.31\, b^*$; these 1D fluctuations become correlated along the c axis below ~ 200 K ; analysis of the temperature dependent intensities of the corresponding superlattice spots [33] lead to assign the CDW condensation temperatures at $T_1 = 150$ K and $T_2 = 105$ K respectively ; moreover, an induced change in the intensity of q_1 when q_2 is condensing, constitutes the signature of a coupling between the two CDWs ; evidence for a strong electron-phonon coupling can be also derived. Finally, these CDWs are associated with the $Pd(dmit)_2$ chains only, i.e. the TTF chain does not seem to be affected [33].

Thus, it seems quite strange that transport measurements could show at 240 K, through the resistivity minimum, some precursor effect to the 1D-2D crossover transition which takes place at 200 K. Even if a close connection cannot be established between these two temperatures, it is worthwhile to emphasize a similar behaviour in orthorombic TaS_3 : an upward resistivity rounding is observed below a resistivity minimum which takes place ~ 50 K above the Peierls transition at 215 K ; this was interpreted as the occurrence of a pseudo-gap due to large CDW fluctuations [34]. On the other hand, the narrow ESR signal which appears below 150 K could be probably related to the commensurate CDW condensation, whereas the inflexion point of the resistivity curve around 110 K should be associated with the incommensurate CDW.

In a pure 1D picture, it is tempting to try to explain these features from the three doubly degenerate and parallel bands scheme derived for metallic $TTF(Ni(dmit)_2)_2$ by tight-binding band structure calculations [35] : if a similar model holds also for α'-$TTF(Pd(dmit)_2)_2$, the Fermi level should cut the donor HOMO TTF band at q_d and the two acceptor LUMO bands at q_{a1} and q_{a2}, respectively ; now, if successive CDWs condense at $2\,q_i$ or $4\,q_i$ ($i = a1, a2$) below the (pressure dependent) temperatures T_1 and T_2, then the respective Fermi surface sheets should disappear, but the FS sheet corresponding to the TTF chain may remain : this must induce some carrier condensations due to the electron-hole pairings and a « metal-semiconducting » like transition, i.e. a metal-semimetal transition, since all the carriers will not be condensed at low temperatures. This can explain why it is difficult to find a classical single activation energy, due to the two successive opening gaps and due to the remaining carriers at low temperatures.

But, even by taking into account i) a larger bandwith, owing to the contracted structure of the Pd salt along b compared to the Ni salt, and ii) different band fillings, i.e. charge transfers from the TTF to the $Pd(dmit)_2$ units, it seems difficult [33, 36] to assign the observed CDWs to the actual published [35] — even modified — band structure. Hence, more sophisticated band structure calculations are presently undertaken, which take into account notably the relative orientation of the molecules (neglected in [35]).

Now, it seems worthwhile to compare the Pd salt with some other 1D compounds, which share similar properties : for example, at 1 bar, the temperature variation of the neutron

diffraction intensities enable to identify a Peierls transition at 120 K in KCP(Br) ; plot of d Log $R/\mathrm{d}(1/T)$ shows a broad extremum 20 K below, and the resistivity curve shows no evident sign of carrier condensation in its continuous upward curvature [37] ; a similar behaviour is observed in cyclo-penta-perylene CPP [38]. But, in both KCP(Br) and CPP materials, the effect of pressure is to increase the Peierls transition temperature. On the other hand, $NbSe_3$ which remains metallic down to 2.5 K at 1 bar, presents two successive opening gaps related to independent and incommensurate CDWs at $T_1 = 145$ and $T_2 = 59$ K. Pressure induces a decrease of these temperatures [34], the initial rate d Ln $T/\mathrm{d}P$ of which is respectively equal to -2.7×10^{-2} and -0.1/kbar ; entrance of the superconductivity is very similar to the Pd salt case, and above 6 kbar, the superconducting temperature T_c decreases with pressure [34] at the same rate as for T_1, since the slope d Ln $T_c/\mathrm{d}P$ is equal to -2.9×10^{-2}/kbar ; this point could significantly tell on which bands set in the corresponding CDW and superconducting competing instabilities. It seems worthwhile to note that the decreasing rate of T_c induced by pressure is very close to the corresponding value derived for the Pd salt.

In conclusion, this study presents a coherent description of the basic physical ingredients which govern the high and low pressure regimes of the α'-TTF(Pd(dmit)$_2$)$_2$ phase diagram : an electron-phonon interaction seems to be at work in the establishment not only of the 3D superconducting condensation, but also of the 1D-2D CDWs instabilities at 1 bar. This constitutes a strong evidence that the phonon mediated electron-electron interaction dominates over the Coulomb one, as in $NbSe_3$ and TaS_3 [39].

Acknowledgments.

It is a pleasure to thank M. Konczykowski for InSb pressure gauges, J. C. Ameline for very high pressure facilities and D. Jerome for his stimulating interest. We acknowledge J. P. Legros for X-ray refinements and H. Hurdequint for ESR measurements. We would also like to thank H. Schulz and P. Garoche for fruitful remarks at different steps of this work. We are indebted to S. Ravy and J. P. Pouget for extensive discussions on 1D instabilities, and to E. Canadell for an illuminating approach of the band structure of the X[(M(dmit)$_2$)]$_2$ family.

References

[1] JEROME D. and SCHULZ H. J., *Adv. Phys.* **31** (1982) 299.
[2] WILLIAMS J. M., WANG H. H., EMGE T. J., GEISER U. R. S., BENO M. A., LEUNG P. C. W., CARLSON K. D., THORN R. J. and SCHULTZ A. J., *Prog. Inorg. Chem.* **35** (1987) 51.
[3] MURATA K., KIKUCHI K., TAKAHASHI T., KOBAYASHI K., HONDA Y., SAITO K., KANODA K., TOKIWA T., ANZAI H., ISHIGURO T. and IKEMOTO I., *J. Mol. Electron.* **4** (1988).
[4] KIKUCHI K., MURATA K., HONDA Y., NAMIKI T., SAITO K., ISHIGURO T., KOBAYASHI K. and IKEMOTO I., *J. Phys. Soc. Jpn* **56** (1987) 3436.
[5] PAPAVASSILIOU G. C., TERZIS A., HILTI B., MAYER C. W. and PFEIFFER J., I.C.S.M. 88 Proc., *Synth. Met.* **27** (1988) B 379.
[6] VALADE L., State Thesis (1987) Toulouse.
[7] BROSSARD L., RIBAULT M., BOUSSEAU M., VALADE L. and CASSOUX P., *C. R. Acad. Sc. Paris II* **302** (1986) 205.
[8] KOBAYASHI A., KIM H., SASAKI Y., KATO R., KOBAYASHI H., MORIYAMA S., NISHIO Y., KAJITA K. and SASAKI W., *Chem. Lett.* **7** (1987) 1819.
[9] BOUSSEAU M., VALADE L., LEGROS J. P., CASSOUX P., GARBAUSKAS M. and INTERRANTE L. V., *J. Am. Chem. Soc.* **108** (1986) 1908.
[10] BANUS M. D. and LAVINE M. C., *J. Appl. Phys.* **40** (1969) 409.

[11] KONCZYKOWSKI M., BAJ M., SZAFARKIEWICZ E., KONCZEWICZ L. and POROWSKI S., High Pressure and Low Temperature Physics (1978) p. 523 (Plenum Press, N.Y.).
[12] LEGROS J. P. and VALADE L., *Solid State Commun.* **68** (1988) 599.
[13] BOUSSEAU M., VALADE L., BRUNIQUEL M. F., CASSOUX P., GARBAUSKAS M., INTERRANTE L. and KASPER J., *Nouv. J. Chim.* **8** (1984) 3.
[14] PAULING L., The Nature of the Chemical Bond (Cornell Univ. Press, Ithaca, N.Y.) 1960.
[15] LEE P. A. and READ N., *Phys. Rev. Lett.* **58** (1987) 2691.
[16] MCMILLAN W. L., *Phys. Rev.* **167** (1968) 331.
[17] TINKHAM M., Introduction to superconductivity (McGraw-Hill) 1975.
[18] MAKI K., *Phys.* **1** (1964) 21 ;
DE GENNES P. G., Superconductivity of Metals and Alloys (Benjamin) 1966.
[19] ORLANDO T. P., MCNIFF E. J., FONER J. R. and S. and BEASLEY M. R., *Phys. Rev. B* **19** (1979) 4545.
[20] BRANDT N. B. and GINZBURG N. I., *Sov. Phys. Uspekhi* **8** (1965) 202.
[21] WHITE R. M. and GEBALLE T. H., Long Range Order in Solids (Acad. Press) 1979.
[22] GAROCHE P., BRUSETTI R. and JEROME D., *J. Phys. Lett. France* **43** (1982) L-147.
[23] BROSSARD L., HURDEQUINT H., RIBAULT M., VALADE L., LEGROS J. P. and CASSOUX P., I.C.S.M. 88, Proc., *Synth. Met.* **27** (1988) B 157.
[24] MOTT N. F., Metal-Insulator Transitions (Taylor & Francis) 1974.
[25] HAMILTON E. M., *Philos. Mag.* **26** (1972) 1043.
[26] BLOCH A. N., WEISMAN R. B. and VARMA C. M., *Phys. Rev. Lett.* **28** (1972) 753.
[27] ALTSHULER B. L., ARONOV A. G. and LEE P. A., *Phys. Rev. Lett.* **44** (1980) 1288.
[28] ABRAHAMS E., ANDERSON P. W., LICCIARDELLO D. C. and RAMAKRISHNAN T. V., *Phys. Rev. Lett.* **42** (1979) 673.
[29] COULON C., DELHAES P., FLANDROIS S., LAGNIER R., BONJOUR E. and FABRE J. M., *J. Phys. France* **43** (1982) 1059 ;
CREUZET F., BOURBONNAIS C., CARON L. G., JEROME D. and BECHGAARD K., *Synt. Met.* **19** (1987) 289.
[30] BOURBONNAIS C., Low Dimensional Conductors and Superconductors (Plenum Press) 1987, p. 155.
[31] SOLYOM J., *Adv. Phys.* **28** (1979) 201 ;
EMERY V. J., BRUINSMA R. and BARISIC S., *Phys. Rev. Lett.* **48** (1982) 1039.
[32] COULON C., Private communication.
[33] RAVY S., POUGET J. P., VALADE L. and CASSOUX P., to be published in *Europhys. Lett.*
[34] MONCEAU P., Electronic Properties of Inorganic quasi 1D compounds, Ed. P. Monceau (D. Reidel Publ. Cie) 1985.
[35] KOBAYASHI A., KIM H., SASAKI Y., KATO R. and KOBAYASHI H., *Solid State Commun.* **62** (1987) 57.
[36] CANADELL E., Private communication.
[37] KUSE D. and ZELLER H. R., *Phys. Rev. Lett.* **27** (1971) 1060 ;
CARNEIRO K., Electronic Properties of Inorganic quasi 1D compounds, Ed. P. Monceau (1985).
[38] PENVEN P., JEROME D., RAVY S., ALBOUY P. A. and BATAIL P., I.C.S.M. 88, Proc., *Synth. Met.* **27** (1989) B 405.
[39] BARISIC S., Electronic Properties of Inorganic quasi 1D compounds. Ed. P. Monceau (1985).